Impact of SVC on the protection of transmission lines

Amir Ghorbani [a,*], Mojtaba Khederzadeh [b], Babak Mozafari [a]

[a] Department of Electrical Engineering, Science & Research Branch, Islamic Azad University, Tehran, Iran
[b] Department of Electrical Engineering, Power & Water University of Technology (PWUT), Tehran, Iran

ARTICLE INFO

ABSTRACT

The impact of Static Var Compensator (SVC) on the apparent impedance seen by the transmission line distance relay is investigated in this paper. Analytical results are presented and verified by detailed simulations. It is shown that the connection type of the windings of the shunt coupling transformer of the SVC has a remarkable effect on the apparent impedance seen by the distance relay. Six different phase to phase and phase to ground measuring units of the distance relay are simulated to resemble the behavior of the relay. The impact of SVC is more pronounced on the apparent impedance seen by the phase to ground fault measuring units than the others as is shown by the results. Simulation results include different power system operating conditions, SVC control system settings and different fault-type scenarios. The impact of SVC on the relay tripping boundaries is also clearly demonstrated. Detailed and sophisticated models are used for simulating distance protective relay in a digital simulation environment.

© 2012 Elsevier Ltd. All rights reserved.

1. Introduction

Static Var Compensator (SVC) is one of the earliest Flexible AC Transmission System (FACTS) devices. It generates or absorbs reactive power at its point of connection, usually in the middle of a high voltage transmission line. Before the evolution of SVC in the 1960s, synchronous compensators performed such compensation. Generally, SVC is used to maintain the voltage magnitude at the middle of a long transmission line, thereby to increase the power transfer capability in a given transmission line. Since SVC cannot generate or absorb real power (neglecting its relatively low internal losses), the power transmission of the system is affected indirectly by the voltage control. SVC regulates the voltage at its terminals by controlling the amount of reactive power injected into or absorbed from the power system. When the system voltage is low, SVC generates reactive power (capacitive mode) and when the voltage is high, it absorb reactive power (inductive mode) [1].

However, the employment of a SVC in a transmission line creates certain problems for the protective relays and fault locators using conventional techniques because of the rapid changes introduced by the associated control actions. Apparent line impedances seen by conventional distance relays are affected due to the variation of the voltage at the point of SVC connection. It is worth noting that distance relays estimate the fault location by calculating the apparent impedance using the voltage and current values at the relaying point [2,3]. When a single a phase fault occurs on a transmission line compensated by SVC; the system voltage decreases, so

the SVC takes remedial actions to recover the voltage to its reference value (V_{Ref}). In this sense, reactive capacitive current is needed to be injected by SVC; therefore, the impedance seen by the distance relay starts to change by the intervention of SVC.

Generally, the impact of compensators on the transmission line protection is categorized as series compensation, shunt compensation and series/shunt compensation. The impact of series compensation on the performance of conventional distance relay is presented in [4–7]. The impact of shunt compensation on conventional distance protection has already been studied in [8–10]; meanwhile the impact of series/shunt compensation devices are reported in [11–14]. In these works, it is shown that the presence of FACTS compensators in a fault loop affects the apparent impedance seen by the distance relay. In [8], the impact of STATCOM is investigated. In [9], the performance of distance relays in presence of shunt FACTS compensation devices, i.e., SVC and STATCOM is presented. The main focus of Sidhu et al. [9] is on the impact of STATCOM on the performance of distance relay.

In this paper, the impact of SVC on the apparent impedance seen by a conventional distance relay is evaluated both analytically and by detailed simulations. The merits of this study are summarized as follows:

(1) The impact of SVC is investigated analytically by applying accurate modeling concepts which is missing in most of the literature in this regard, then the analytical results are verified by detailed simulations.
(2) Sophisticated models are used for sources, transmission lines, protective relay and other devices in the sample network.

* Corresponding author.
   E-mail address: AmirGhorbani@stud.pwut.ac.ir (A. Ghorbani).

(3) SVC control system is simulated by detailed transient models. Static models for SVC, as used in some published papers, does not accurately present the behavior of SVC during a fault; hence the performance of the distance relay is not clearly evaluated in this case.

(4) The impact of SVC on the trip boundaries of the distance relay is investigated and interesting results are provided.

(5) In this paper, it is shown that the connection type of the windings of the SVC's coupling transformer directly affects the behavior of the relay.

2. Sample system modeling

Fig. 1 shows the sample system used for the study. It contains two parallel 300 km, 230 kV transmission lines, with the SVC installed in the middle of Line 1. The positive sequence line impedances are the same and equals $Z_{1L1} = Z_{1L2} = 0.0255 + j0.3520\ \Omega/$km; the zero sequence line impedances are $Z_{0L1} = Z_{0L2} = 0.3864 + j1.5556\ \Omega/$km. Short Circuit Level (SCL) at G and H = 8500 MVA; system frequency = 60 Hz; load angle between sources = 30° and the ratio between the magnitudes of the source voltages at G and H = 1.07.

The SVC considered contains one 100 Mvar TCR bank and three 100 Mvar TSC banks which are connected to the middle of Line 1 using a 230 kV/16 kV (Yg/d), 340 MVA coupling transformer. Each three-phase bank is connected in delta so that, during normal balanced operation, the zero-sequence triplen harmonics (3rd, 9th, etc.) remain trapped inside the delta, thus reducing harmonic injection into the power system. Switching the TSCs in and out allows a discrete variation of the secondary reactive power from zero to 300 Mvar capacitive (at 16 kV) by steps of 100 Mvar, whereas phase control of the TCR allows a continuous variation from zero to 100 Mvar inductive.

SVC control system is presented in Fig. 2. Positive sequence fundamental-frequency primary voltage magnitude $V_{abc}(Prim)$, is measured by voltage measurement unit and then is compared with V_{Ref}. The obtained error passes through a PI regulator and presents the primary susceptance, B_{svc}. The associated Phase Locked Loop (PLL) is used to take into account the variations of the system frequency. Distribution unit in Fig. 2 uses B_{svc} to determine the TCR firing angle α and the status (on/off) of the three TSC branches. The firing angle α as a function of the TCR susceptance B_{TCR} is implemented by a look-up table extracted from:

$$B_{TCR} = \frac{2(\pi - \alpha) + \sin(2\alpha)}{\pi} \tag{1}$$
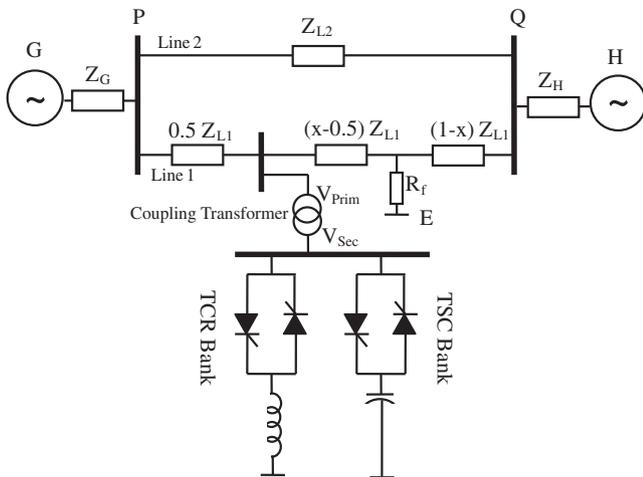
Fig. 1. Single line diagram of the sample system.
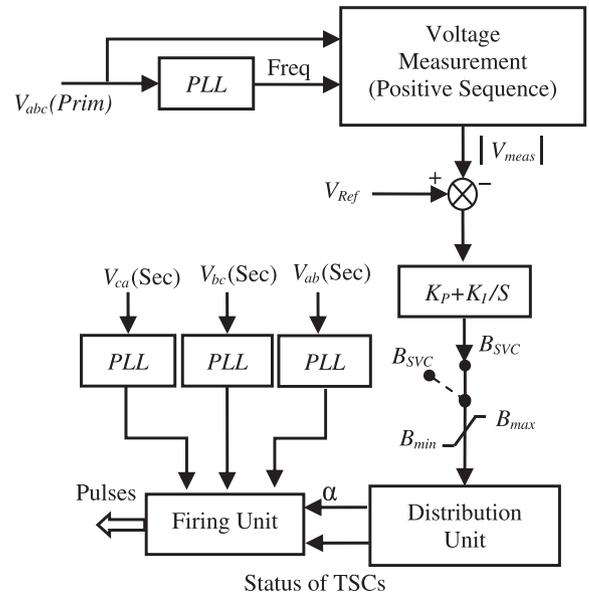
Fig. 2. SVC control system.

where B_{TCR} is the TCR susceptance in p.u. of rated TCR reactive power (100 Mvar). A synchronizing system using a three PLLs synchronized on line-to-line secondary voltages $V_{abc}(Sec)$, and a pulse generator that send appropriate pulses to the 24 thyristors (six thyristors per three-phase bank) are the main components of this SVC control system.

Generally, SVC has two different operational modes:

(1) Voltage regulation mode: In this case V_{Ref} value is specified by external controller. SVC holds output voltage in V_{Ref} by absorbing or generating reactive power and it is performed by a PI regulator.

(2) Var regulation mode: SVC reactive power is fixed in this case and the SVC susceptance is kept constant. The presence of voltage regulator is not necessary in the control system in this mode, so B_{SVC} is applied directly by external controller to the SVC.

3. SVC impact on the apparent impedance measured by the distance relay

Fig. 3 shows the positive, negative and zero-sequence networks of the sample system of Fig. 1 with the SVC in the middle of Line 1. Distance relay is installed at Bus P to protect the associated transmission line. Following parameters are used for the analysis:

V_{0p}, V_{1p}, V_{2p}	are sequence phase voltages at relay location at Bus P;
$I_{0p1}, I_{1p1}, I_{2p1}$	are sequence phase currents through Line 1 at relay location at Bus P;
$I_{0p2}, I_{1p2}, I_{2p2}$	are sequence phase currents through Line 2 at relay location at Bus P;
$I_{0q1}, I_{1q1}, I_{2q1}$	are sequence phase currents through Line 1 at Bus Q;
V_{0E}, V_{1E}, V_{2E}	are sequence phase voltages at fault location E;
$Z_{0s1}, Z_{1s1}, Z_{2s1}$	are sequence impedances of the Line 1;
$Z_{0s2}, Z_{1s2}, Z_{2s2}$	are sequence impedances of the Line 2;
R_f	is fault resistance;
x	is fault per-unit distance from the relay location.

Fig. 3. (a) Positive sequence network. (b) Negative sequence network. (c) Zero sequence network.

For positive sequence network according to Fig. 3, following equations can be derived for Lines 1 and 2 for a fault at B with the fault resistance R_f:

$$V_{1p} = xZ_{1s1}I_{1p1} + (x - 0.5)Z_{1s1}I_{1sh} + R_f(I_{1p1} + I_{1sh} + I_{1q1}) + V_{1E} \qquad (2)$$

$$V_{1p} = Z_{1s2}I_{1p2} + (1 - x)Z_{1s1}I_{1q1} + R_f(I_{1p1} + I_{1sh} + I_{1q1}) + V_{1E} \qquad (3)$$

Extracting V_{1E} from (3) and replacing it in (2) we have:

$$I_{1q1} = \frac{x}{(1-x)}I_{1p1} + \frac{(x-0.5)}{(1-x)}I_{1sh} - \frac{k_1}{(1-x)}I_{1p2} \qquad (4)$$

where

$$k_1 = Z_{1s2}/Z_{1s1} \qquad (5)$$

By substituting (4), in (2), the following equation is obtained:

$$V_{1p} = xZ_{1s1}I_{1p1} + (x - 0.5)Z_{1s1}I_{1sh}$$
$$+ R_f\left(\frac{1}{(1-x)}I_{1p1} + \frac{0.5}{(1-x)}I_{1sh} - \frac{k_1}{(1-x)}I_{1p2}\right) + V_{1E} \qquad (6)$$

The negative and zero sequence voltages are obtained from Fig. 3 in the same way:

$$V_{2p} = xZ_{1s1}I_{2p1} + (x - 0.5)Z_{1s1}I_{2sh}$$
$$+ R_f\left(\frac{1}{(1-x)}I_{2p1} + \frac{0.5}{(1-x)}I_{2sh} - \frac{k_1}{(1-x)}I_{2p2}\right) + V_{2E} \qquad (7)$$

$$V_{0p} = xZ_{0s1}I_{0p1} + (x - 0.5)Z_{0s1}I_{0T}$$
$$+ R_f\left(\frac{1}{(1-x)}I_{0p1} + \frac{0.5}{(1-x)}I_{0T} - \frac{k_0}{(1-x)}I_{0p2}\right) + V_{0E} \qquad (8)$$

where

$$k_0 = Z_{0s2}/Z_{0s1} \qquad (9)$$

3.1. Single phase to ground fault

For a single phase to ground fault (L–G) following equations can be used:

$$V_{0E} + V_{1E} + V_{2E} = 0 \qquad (10)$$

By using 6, 7, 8, and (10) we have:

$$V_{L-G} = x[Z_{1s1}I_{p1} + (Z_{0s1} - Z_{1s1})I_{0p1}]$$
$$+ \frac{R_f}{(1-x)}[I_{p1} - K_1I_{p2} + (K_1 - K_0)I_{0p2}] + \Delta V_{L-G} \qquad (11)$$

where

$$V_{0p1} + V_{1p1} + V_{2p1} = V_{L-G} \qquad (12)$$

$$I_{0p1} + I_{1p1} + I_{2p1} = I_{p1} \qquad (13)$$

$$I_{0p2} + I_{1p2} + I_{2p2} = I_{p2} \qquad (14)$$

$$I_{0T} + I_{1sh} + I_{2sh} = I_{sh} \qquad (15)$$

and

$$\Delta V_{L-G} = (x - 0.5)Z_{1s1}I_{sh} + (x - .05)(Z_{0s1} - Z_{1s1})I_{0T}$$
$$+ \frac{R_f}{(1-x)}I_{sh} \qquad (16)$$

For a single phase to ground fault, the apparent impedance is obtained by using the above equations:

$$Z_{L-G} = \frac{V_{L-G}}{I_{p1} + [(Z_{0s1} - Z_{1s1})/Z_{1s1}]I_{0p1}} = \frac{V_{L-G}}{I_{L-G}} \qquad (17)$$

From (11) and (17) we have:

$$Z_{L-G} = xZ_{1s1} + \frac{R_f}{(1-x)I_{L.G}}[I_{p1} - k_1I_{p2} + (k_1 - k_0)I_{0p2}] + \Delta Z_{L-G} \qquad (18)$$

When there is no shunt compensation ΔZ_{L-G} in (18) is zero and the apparent impedance is the same as uncompensated lines, so ΔZ_{L-G} depends on the shunt compensator and equals:

$$\Delta Z_{L-G} = (x - 0.5)Z_{1s1}\frac{I_{sh}}{I_{L-G}} + (x - 0.5)(Z_{0s1} - Z_{1s1})\frac{I_{0T}}{I_{L-G}}$$
$$+ R_f\frac{0.5}{(1-x)}\frac{I_{sh}}{I_{L-G}} \qquad (19)$$

It can be deduced from (19) that the presence of shunt compensator in the fault loop affects the calculated impedance by the relay. When the fault distance from the relay is 0.5 p.u. or the shunt compensator is not present in the fault loop, its effect on the impedance Z_{L-G} is only through R_f.

3.2. Phase to phase fault

For a phase to phase fault (L–L) we have:

$$V_{1E} = aV_{2E} \qquad (20)$$

where

$$a = -0.5 + j0.886 \qquad (21)$$

From (6), (7), and (20) we have:

$$V_{1p} - aV_{2p} = xZ_{1s1}(I_{1p1} - aI_{2p1}) + (x - 0.5)Z_{1s1}(I_{1sh} - aI_{2sh})$$
$$+ \frac{R_f}{(1-x)}[(I_{1p1} - aI_{2p1}) + 0.5(I_{1sh} - aI_{2sh})$$
$$+ k_1(aI_{2p2} - I_{1p2})] \qquad (22)$$

The apparent impedance for a phase to phase (L–L) fault is as:

$$Z_{L-L} = \frac{V_{1p} - aV_{2p}}{I_{1p1} - aI_{2p1}} = \frac{V_{1p} - aV_{2p}}{I_{L-L}} \qquad (23)$$

By replacing (22) in (23), we have:

$$Z_{L-L} = xZ_{1s1} + \frac{R_f}{(1-x)I_{L-L}}[(I_{1p1} - aI_{2p1}) + k_1(aI_{2p2} - I_{1p2})]$$
$$+ \Delta Z_{L-L} \qquad (24)$$

In above equation, ΔZ_{L-L} depends on presence shunt compensator and it is equal to:

$$\Delta Z_{L-L} = (x - 0.5)Z_{1s1}\frac{(I_{1sh} - aI_{2sh})}{I_{L-L}} + \frac{0.5R_f}{(1-x)I_{L-L}}(I_{1sh} - aI_{2sh}) \qquad (25)$$

In above equation R_f is the fault resistance between two phases. According to (25) for $R_f = 0$, the shunt compensator impact is due to the negative and positive sequence current differences.

4. Simulation results

The simulation is performed by using MATLAB/Simulink software environment with SimPowerSystems toolbox and the Simulink library [15].

4.1. Distance relay modeling

The distance relay model is developed according to (17) for L–G faults and (23) for L–L faults, where three phase voltages and currents are passed through anti-aliasing low-pass filters [3], then the phasors are extracted using Full Cycle Discrete Fourier Transform (FCDFT). Finally, after calculation the positive, negative and zero sequence components of the estimated phasors, the apparent impedances for the six measuring units (A–G, B–G, C–G, A–B, B–C, and C–A) are evaluated [2,3].

4.2. Single phase to ground fault

AC system voltages are normally balanced and therefore compensators normally control all three phases of their output current together. This means the SVC control system normally establishes three identical shunt admittances, one per each phase. Consequently with unbalanced system voltages the compensating currents in each phase would become different. It is possible to control the three compensating admittances individually by adjusting the delay angle of the TCRs so as to make the three compensating currents identical. However, in this case the triplen harmonic content would he different in each phase and their normal cancellation through delta connection would not take place. Thus, this operation mode would generally require the installation of the usually-unnecessary third harmonic filters. For this reason, individual phase control for SVCs in transmission line compensation is rarely employed [1]. Therefore, SVC is unable to equally compensate all the three phases during L–G faults. Fig. 4 shows the SVC three phase currents, for an L–G fault (A–G) occurred at 0.4 s at 225 km from the relay. According to Fig. 4, after the A–G fault, SVC is unable to equally compensate all the three phases, hence, all the three phases of the SVC output currents are going to have the same phases. Therefore, the zero-sequence component of the injected current (I_{0T}) increases. According to (19), this current has a direct impact on the apparent impedance. Apparent impedance seen by the A–G measuring unit of the relay for the same A–G fault is shown in Fig. 5. As can be deduced from this figure, presence of SVC in the fault loop and its injected capacitive current, forces the relay to under-reach. According to the analytical analysis, SVC effect in the impedance Z_{L-G} is due to ΔZ_{L-G} as in (19), where the imaginary and real parts are extracted for this A–G fault and is shown in Fig. 6. Comparing the results of Figs. 5 and 6 indicates the consistency between the simulation results and the theoretical analysis presented in the previous section.

In order to demonstrate the effect of I_{0T} on the apparent impedance seen by the distance relay, the connection type of the SVC coupling transformer could be selected in such a way as to nullify the impact of I_{0T}. For example, the transformer primary connection could be changed from Yg to Y. The same results are simulated and shown in Fig. 7 for the same A–G fault for this new connection; it can be clearly deduced that the SVC impact is diminished significantly.

In the model of SVC, TSC branch is used instead of Fixed Capacitor (FC). For investigating the effect of SVC on distance relay, it could be deduced that the TSC or the FC as part of the SVC, has no significant difference, because during the fault the SVC generates all its reactive power to compensate the voltage
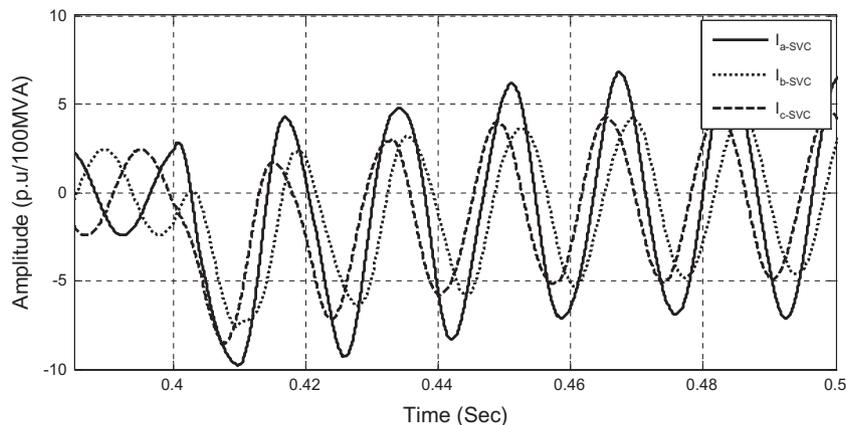
Fig. 4. SVC three phase currents, for an L–G fault (A–G) occurred at 0.4 s at 225 km from the relay.
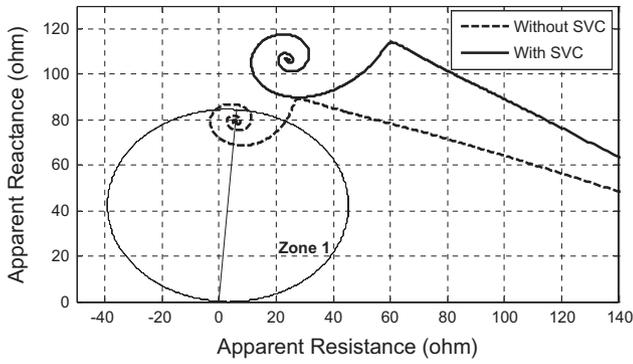
Fig. 5. Apparent impedance calculated by the A–G measuring unit of the relay for an A–G fault occurred 225 km from the relay.

Fig. 6. Imaginary and real parts of ΔZ_{L-G} for an A–G fault occurred at 0.4 s at 225 km from the relay.

Fig. 7. Apparent impedance calculated by the A–G measuring unit of the relay for an A–G fault occurred at 225 km from the relay.

Fig. 8. Apparent impedance calculated by the A–B measuring unit of the relay for an A–B fault occurred 225 km from the relay.
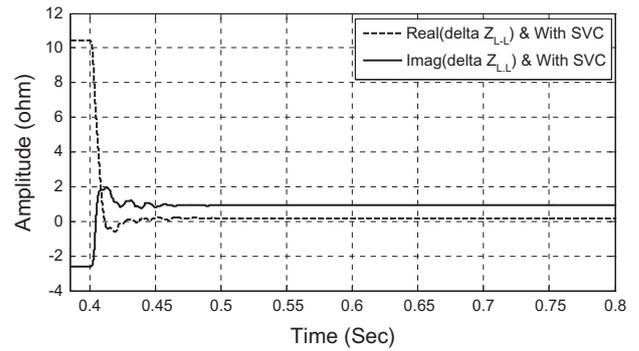
Fig. 9. Imaginary and real parts of ΔZ_{L-L} for an A–B fault occurred at 0.4 s at 225 km from the relay.
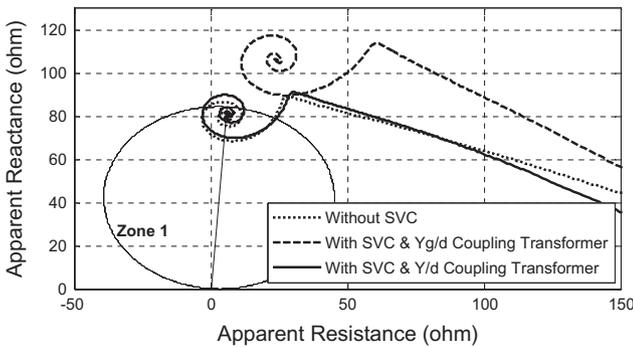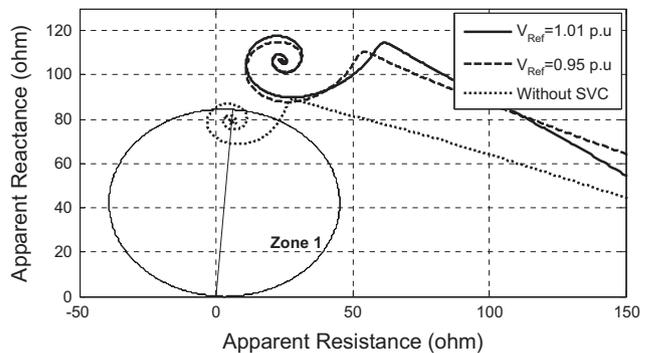
Fig. 10. Apparent impedance calculated by the A–G measuring unit of the relay for an A–G fault occurred at 225 km from the relay for different reference voltages.

drop at the fault point. It means TSC will be fully utilized and thereby, thyristors will be short circuited, hence, converting the TSC to FC.

4.3. Phase to phase fault

For an A–B fault at 225 km from the relay, the apparent impedance calculated by A–B measuring unit is presented in Fig. 8, which shows that the presence of SVC in the fault loop does not have an appreciable impact. Real and imaginary parts of ΔZ_{L-L} as (25) are shown in Fig. 9. As can be deduced from this figure, the effect of phase to phase faults on the apparent impedance is negligible. The simulation results are in good companion with the analysis presented by (25).

4.4. The effect of SVC setting

Figs. 10 and 11 show the apparent impedance and reactive power injected by SVC for an L–G fault (A–G) occurred at 0.4 s at 225 km from the relay when the SVC voltage settings (V_{Ref}) are 0.95 and 1.01 p.u., respectively. As can be seen from Fig. 10, SVC will have the same effect in calculated impedance by the relay for different V_{Ref} values. After inception of an A–G fault, SVC reactive power injection is the same for both V_{Ref} values. In other words, whether SVC injects reactive power ($V_{Ref} = 1.01$), or absorbs reactive power ($V_{Ref} = 0.95$) before a fault, it will inject the same value of reactive power after the fault. This SVC behavior is justifies as follows:

After inception of an A–G fault in any pre-specified V_{Ref} value, the measured SVC positive-sequence voltage $|V_{meas}|$ is less than
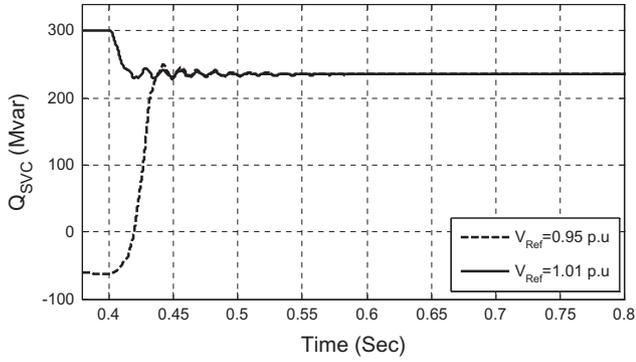
Fig. 11. Reactive power compensation of SVC with different SVC setting for an A–G fault occurred at 0.4 s at 225 km from the relay.

Fig. 14. Trip characteristic without SVC for A–G fault.

Fig. 12. Apparent impedance calculated by the A–G measuring unit of the relay for an A–G fault occurred at 225 km from the relay for different short-circuit levels.
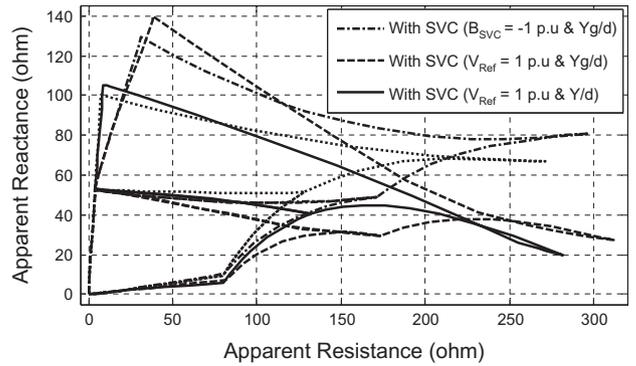
Fig. 15. Trip characteristic with/without SVC for an A–G fault.

Fig. 13. Apparent impedance calculated by the A–G measuring unit of the relay for an A–G fault occurred at 225 km from the relay for different load angles.
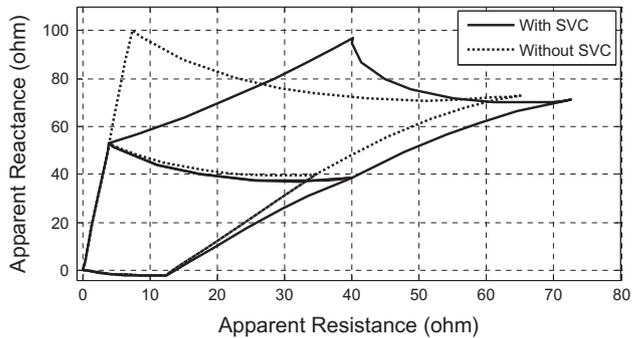
Fig. 16. Trip characteristic calculated by the A–G measuring unit with/without SVC for an A–B–G fault.

V_{Ref}, therefore, SVC should inject reactive power to increase $|V_{meas}|$ to the V_{Ref} value.

4.5. The effect of system Short Circuit Level (SCL) and load angle

Fig. 12 shows apparent impedance calculated by A–G measuring unit for an A–G fault occurred at 225 km from the relay and different system SCLs with presence of SVC. As can be seen from Fig. 12, the impact of SVC on the apparent impedance is significant for weak systems and this impact is more pronounced on the apparent reactance. This is due to the fact that fault currents are lower for weak systems in comparison to the strong systems. Therefore in systems with small SCL, the SVC injected capacitive currents are appreciable in comparison to the fault currents. For

different load angles and the same A–G fault, the impact of SVC on the apparent impedance calculated by the A–G measuring unit is shown in Fig. 13. As can be seen from this figure, SVC increases the R/X value by increasing the load angle.

4.6. Trip characteristics

The trip characteristics of the relay is obtained by keeping the system operating conditions constant, while the fault location (0–95% of the length of transmission Line 1) and fault resistance R_f (from 0 to 200 Ω) are varied [12].

4.6.1. Single phase to ground fault

Fig. 14 shows the trip characteristics without the presence of SVC calculated by the A–G measuring unit. SVC effect on the trip characteristics is shown in Fig. 15. According to this figure, the presence of shunt compensator in the middle of the Line 1 caused
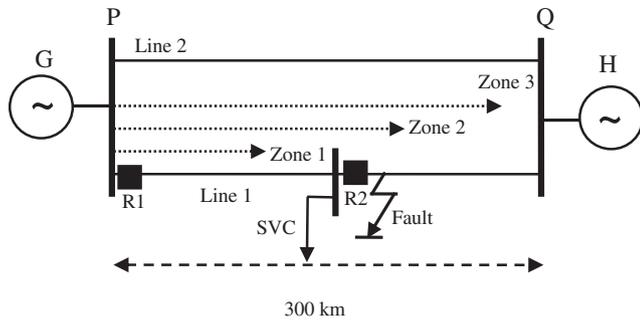
Fig. 17. Single line diagram of the sample system 2.

the trip characteristics to be split into two parts. The lower part is for faults that occur at 0–50% of Line 1 for R_f varying from 0 to 200 Ω. According to the presented analysis, SVC effect on the apparent impedance for these faults depends on the value of R_f, i.e., for $R_f = 0$ Ω the SVC has no effect, so by increasing R_f, the impact of compensator increases; which can be also deduced from the simulation results presented in Fig. 15. The upper part is related to the faults between the middle of Line 1 to 95% of the line length with the presence of SVC in the fault loop. Fig. 15 also indicates that for A–G faults with low R_f values, SVC increases both apparent resistance and reactance; while for high R_f values, SVC mainly decreases the apparent reactance in the voltage regulation mode (V_{Ref} = 1 p.u.) and mainly increases the apparent reactance in Var regulation mode (absorbing reactive power) (B_{SVC} = −1). According to Fig. 15 the impact of SVC with Y/Δ coupling transformer on the apparent impedance for A–G faults with low R_f values is mitigated.

4.6.2. Double phase to ground fault (L–L–G)

For double phase to ground fault A–B–G, the trip characteristics that is calculated by A–G measuring unit is shown in Fig. 16. As can be seen from Fig. 16 like the case in which A–G fault occurs, the presence of SVC in the fault loop affects the apparent impedance (mainly the apparent resistance) calculated by A–G measuring unit.

4.7. The impact of SVC on the back-up relays

In order to analyze the impact of the SVC on the back-up protective relays upon failure of the primary distance relay, another sample system is designed and simulated. Fig. 17 shows the sample system. In this system, Relay R2 is the main relay and R1 is the back-up of R2. For investigation, a single-phase fault is imple-
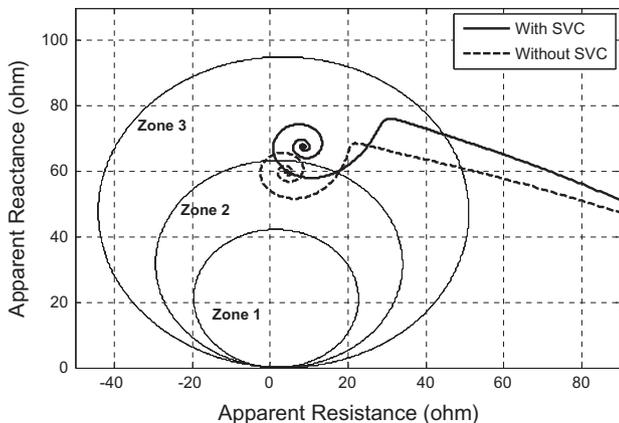
Fig. 18. Apparent impedance calculated by the A–G measuring unit of the R1 for an A–G fault occurred at 170 km from the R1.
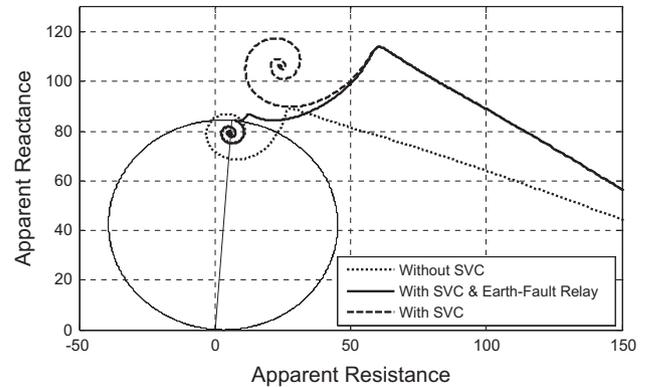
Fig. 19. Apparent impedance calculated by A–G relay element with SVC and earth-fault relay.

mented at 20 km from R2 and 170 km from R1, i.e., at Zone I of R2 and Zone II of R1. Fig. 18 shows the simulation results for the system with/without SVC. As can be deduced from Fig. 18, the SVC impact on the back-up relay is under-reaching of R2, meaning the fault at Zone II without SVC is seen at Zone III with SVC. The SVC impacts on relay R2 to measure the apparent impedance more than the apparent impedance to the fault point. This result is consistent with the analytical results.

5. Remedial action

According to the presented analysis and simulation, the SVC impact on the calculated impedance by the relay is only significant for single phase-to-ground faults. It is also shown that this happens due to the zero-sequence component of the injected current by the SVC. If the SVC is bypassed during the time that the zero-sequence component of the SVC current is increased, then SVC would have no effect on the apparent impedance. In order to recognize the zero-sequence component of the SVC current, an earth-fault relay could be used in the SVC current path [16]. The impedance calculated by the distance relay for the same A–G fault and using an earth-fault relay in the SVC current path to detect and bypass the SVC is shown in Fig 19. It can be seen that the SVC has no remarkable effect on the calculated impedance.

6. Conclusions

In this paper, it is shown that the impact of SVC is more pronounced on the apparent impedance seen by the phase to ground fault measuring units than the phase to phase units. This is due to the zero-sequence current of the SVC coupling transformer primary connection (I_{0T}). If the winding connection of the SVC coupling transformer is changed from Yg/Δ to Δ/Yg or Y/Δ, then the zero-sequence current in the primary connection of the coupling transformer would be zero, so the impact of SVC on the apparent impedance for an A–G fault with low R_f values is mitigated. From the results described in this paper, it can be observed that the trip boundaries of the phase to ground fault measuring units of the relay are influenced by the presence of the SVC. Therefore, to provide a suitable trip boundary for the phase to ground fault measuring units of the relay, the boundary needs to be adaptively manipulated with the zero-sequence current in the primary connection of the coupling transformer of the SVC.

References

[1] Hingorani NG, Gyugyi L. Understanding FACTS concepts and technology of flexible AC transmission systems. New York: IEEE Press; 2000.

[2] Liao Y, Elangovan S. Digital distance relaying algorithm for first-zone protection for parallel transmission lines. IEE Proc – Gener Transm Distrib 1998;145(5):531–6.

[3] Waikar DL, Elangovan S, Liew AC. Fault impedance estimation algorithm for digital distance relaying. IEEE Trans Power Deliv 1994;9(3): 1375–83.

[4] Khederzadeh M, Sidhu TS. Impact of TCSC on the protection of transmission lines. IEEE Trans Power Deliv 2006;21(1):80–7.

[5] Khederzadeh M, Ghorbani A, Salemnia A. Impact of SSSC on the digital distance relay. IEEE/PES general meeting 2009, Calgary, Alberta.

[6] Dash PK, Pradhan AK, Panda G, Liew AC. Digital protection of power transmission lines in the presence of series connected FACTS devise. In: Proc IEEE power engineering soc winter meeting, vol. 3; January 23–27, 2000. p. 1967–72.

[7] Kazemi A, Jamali S, Shateri H. Effect of SSSC on distance relay tripping characteristic. In: Proc first international power and energy conference PECon, Putrajaya, Malaysia; November 28–29, 2006. p. 623–8.

[8] El-Arroudi K, Joos G, McGillis DT. Operation of impedance protection relays with the STATCOM. IEEE Trans Power Deliv 2002;17(2):381–7.

[9] Sidhu TS, Varma RK, Gangadharan PK, Albasri FA, Ortiz GR. Performance of distance relays on shunt—FACTS compensated transmission lines. IEEE Trans Power Deliv 2005;20(3):1837–45.

[10] Khederzadeh M, Ghorbani A. STATCOM modeling impacts on performance evaluation of distance protection of transmission lines. Euro Trans Electr Power 2011(8):2063–79.

[11] Zhou X, Wang H, Aggarwal RK, Beaumont P. Performance evaluation of a distance relay as applied to a transmission system with UPFC. IEEE Trans Power Deliv 2006;21(3):1137–47.

[12] Dash PK, Pradhan AK, Panda G, Liew AC. Adaptive relay setting for flexible AC transmission systems (FACTS). IEEE Trans Power Deliv 2000;15(1):38–43.

[13] Dash PK, Pradhan AK, Panda G. Distance protection in the presence of unified power flow controller. Electr Power Syst Res 2000;54:189–98.

[14] Khederzadeh M, Ghorbani A. Impact of VSC-based multiline FACTS controllers on distance protection of transmission lines. IEEE Trans Power Deliv 2012; 27(1):32–9.

[15] SimPowerSystems toolbox ver. 5.1, for use with Simulink. User's guide 2009. The MathWorks, Inc., Natick, MA

[16] Power system protection, vol. 2. Edited by The Electricity Training Association.